

Two-Modes Dynamics in Dispersed Systems : the Case of Particle-Stabilized Foams Studied by Diffusing Wave Spectroscopy

Antonio Stocco^{1†}, Jérôme Crassous^{2‡}, Anniina Salonen¹,
Arnaud Saint-Jalmes², Dominique Langevin¹

¹Laboratoire de Physique des Solides, UMR CNRS 8502, Université
Paris-Sud, 91405 Orsay cedex, France.

²Institut de Physique de Rennes, UMR CNRS 6251, Université Rennes 1, 35042
Rennes cedex, France

Abstract

The stabilization of aqueous foams solely by solid particles is an active field of research. Thanks to controlled particle chemistry and production devices, we are able to generate large volumes of such foams. We previously investigated some of their unique properties, especially the strongly reduced coarsening. Here we report another type of study on these foams : performing Diffusing Wave Spectroscopy, we can investigate for the first time the internal dynamics at both the scales of the particles and of the bubbles. When compared to surfactant foams, unusual features are observed ; in particular, two well-separated modes are found in the dynamics, both evolving with foam aging. We propose an interpretation of these specificities, taking into account both the scattering by free particles in the foam fluid (fast mode), and by the foam structure (slow mode). To validate our interpretation, we show that independent measurements of the interstitial fluid scattering length, obtained indirectly on the foam and directly on the drained liquid, are in good agreement. As well, we have identified the experimental conditions required to observe such two-processes dynamics : counter-intuitively, the fraction of free particles within the foam interstitial fluid has to be very low to get an optimal signature of these particles on the DWS correlation curves. This study also sheds light on the partitioning of the particles inside the foams and at the interfaces, as the foam ages. Lastly, the results shown here (obtained by analyzing the fluctuations of the transmitted light) implement the previous ones (obtained by analyzing the mean transmitted intensity), and prove that the foam structure is actually not fully frozen.

† Present address : Max Planck Institute of Colloids and Interfaces, Golm, Germany

‡ Author for correspondence

1 Introduction

A dispersion of a gas inside a liquid becomes a foam only if stabilizing agents get adsorbed at the gas-liquid interfaces. The adsorbed layers provide repulsive forces which stabilize the thin liquid films separating the bubbles, keeping them apart. Usual stabilizers are low molecular weight surfactants. An active field of research concerns new types of stabilizers enabling the development of other types of foams and/or to suit specific applications. For instance in food products, proteins efficiently replace surfactants at interfaces [1, 2] ; in other applications, amphiphilic oligomers or polymers are used. The use of solid particles, with diameters ranging from tens of nanometers to microns, is another method which has received a lot of interest in the last years.

Solid particles are expected to act very differently from low molecular weight surfactants at interfaces [3, 4, 5]. In particular, partially because of their sizes, the adsorption at interface can be considered irreversible [4, 5], thus providing high interfacial elasticity, even for slow deformations. However, a major drawback is the difficulty in adsorbing such large particles at gas-liquid or liquid-liquid interfaces. This requires both the use of high energy mixing processes, and optimization of the particle wetting properties [3, 4, 5]. Nevertheless, liquid-liquid dispersions (emulsions) stabilized by solid particles have been produced and studied for years, and are called Pickering emulsions [3, 6, 8]. For these emulsions, macroscopic signatures of the irreversible adsorption of the particles at interfaces are both the arrest of the coarsening process (which otherwise results in the continuous increase of the droplet diameter), and a limited-coalescence effect [7, 8].

In contrast to emulsions, much less has been done on 3D foams solely stabilized by particles [9, 10, 11, 12, 13]; however, single gas-liquid interfaces and isolated bubbles covered by particles have been studied, evidencing new behavior also directly linked to the almost-zero rate of desorption of the particles [5, 14, 15, 16, 17, 18, 19, 20].

Combining progresses both on the particle chemistry and on the foam production method, large volumes of controlled foam have been obtained [13]. In this previous work, we particularly focused on the specificities brought by the particles on the foam aging. Aqueous foams are indeed unstable dispersions ; they evolve in time by drainage (due to gravity), by coarsening (resulting from gas diffusion from bubbles to bubbles), and bubble coalescence. These effects depend both on the physical and chemical parameters of the foam [21]. Coupling optical measurements - based on the average value of the light intensity transmitted through the foam [22] - and a rotating device to avoid drainage, we found clear evidence of a huge reduction of the foam coarsening above a critical concentration of particles, leading to ultrastable foams [13]. This macroscopic behavior was discussed in terms of the high interfacial elasticity, and linked to studies at the gas-liquid interface [19]. In addition, the particles have an effect on the foam drainage. The use of particles does not avoid

the foam drainage: with time, these foams get dryer, but the drainage is extremely slow and a significant amount of liquid always remains trapped inside the foam.

The only tiny increase of the light intensity transmitted through such foams has been interpreted as an almost-complete arrest of coarsening, and a mean bubble size which is constant with time [13]. We can then wonder if the whole bubble structure gets eventually fully frozen, without any usual internal dynamics driven by coarsening. In order to get more information on these foams, at the scale of the bubble, the multiple light scattering technique called Diffusing Wave Spectroscopy (DWS) is a useful tool for measuring dynamics inside turbid media [23, 24]. Previous works have shown that it is very well-suited for foams, where the dynamics observed arise from coarsening-induced bubble rearrangements (at rest), or from bubble motions induced by a macroscopic deformation [25, 26]. Here, in the case of no internal dynamics, one can wonder what could be measured by performing DWS. Moreover, the foaming fluid itself scatters light because of the particles. Light propagation inside such foams could be affected by the dynamics of the particles themselves, as we are in the case of light scattering by a turbid liquid confined inside a scattering matrix. In fact, previous works on light scattering on fluid-infiltrated granular materials showed that even traces of free particles inside the interstitial fluid have an impact, and that non-trivial dynamics can be observed [27]. Here, in good agreement with that previous study, we show that multiple light scattering through these foams is actually different from that observed on surfactant foams. In particular, we show that two distinct dynamic processes are detected, and that the non-classical fast dynamics can be fully explained by the presence of free particles still moving inside the foam interstitial fluid, despite a very low concentration of these particles.

2 Experimental section : materials and methods

2.1 Silica nanoparticles

Silica nanoparticles were kindly provided by Wacker-Chemie (Germany) and were used as received. They are made out of fumed silica, in which, during synthesis, the elementary nanoparticles (spherical-like objects of approximately 20 nm diameter) are fused into fractal aggregates. In the following and for clarity, we will use the name *particle* when considering an aggregate/cluster of nanoparticles. The surfaces of the nanoparticles were modified by reaction of the surface silanol groups with dichlorodimethylsilane. In this study we use particles with a relative SiOH content of 34% which leads to the highest foam stability and foamability (defined as maximum volume of foam obtained after production). Using dynamic light scattering methods [28, 29], it has been found that particle sizes range from 100-500 nm [13, 30, 31]. The particle shape is approximately spherical, and the polydispersity quite low (around

20%).

The dispersions were prepared by adding the amorphous fumed silica powder into water up to a final bulk concentration $c = 0.7$ wt.%, while using a low amount (2 wt.%) of ethanol in the first stages to facilitate particle wetting by water. The dispersion was sonicated for one hour using an ultrasonic probe (Ultrasonic Processor) operating at 20 kHz with 70% of the maximum amplitude in order to obtain a stable dispersion and to break the largest particle aggregates. Note that no surfactants are added.

2.2 Turbulent mixing and foam parameters

We produced large amounts of uniform particle-stabilized foams thanks to a turbulent mixing apparatus, described in [32]. The production rate is high (up to 10 L/min), and by monitoring the gas and liquid rates, one can tune the production rate and the foam liquid fraction, ϕ_l . For low molecular weight surfactant solutions, we can then produce any liquid fraction from $\phi_l = 0.03$ to 0.5.

Here, the foamability of the particle dispersions is not ideal as the particles do not adsorb easily, even with this vigorous mixing process. As a consequence, tuning the initial liquid fraction is less easy (typical liquid fractions ϕ_l are only from 0.15 to 0.3).

Concerning the bubble sizes, measuring the distribution of their diameters remains a difficult task, and only images of the first layer of bubbles in contact with a transparent wall can be easily obtained. From such image analysis and for low molecular weight surfactant solutions, the mean bubble diameter D usually ranges from 70 to 120 microns, depending on the solution used, its foamability and the setup parameters. we usually found that the foams produced are then slightly polydispersed, with a polydispersity typically similar to the one of shaving foams [25]. Here, with the particles, the distribution of diameters appears larger than for usual surfactant solutions and the mean diameter is also more sensitive to the apparatus setup and to solution preparation protocol. In that respect, the initial mean bubble diameter D is typically measured between 60 to 100 microns, with no initial diameters smaller than 25-30 microns and higher than 250 microns.

The outlet tube of the foam generator can be connected to different experimental cells, with different geometries depending on the type of experiments performed. Measurements are either performed in small glass cells, of thickness 1 - 3 cm, or in Plexiglas boxes of height $h = 300$ mm, width $w = 125$ mm, thickness $L = 25$ mm. The vertical position of the measurement (with respect to the top of the foam sample) can then be adjusted. All the experiments described in the paper were performed at room temperature (~ 22 °C).

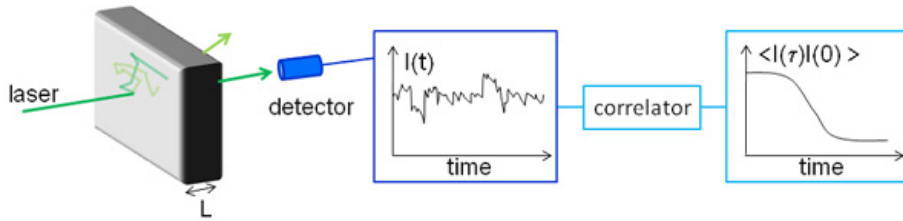


Figure 1: A schematic drawing of the DWS setup

2.3 Light scattering techniques

Diffusing wave spectroscopy (DWS) is becoming a rather classical technique for investigating turbid media [23, 24]; though the setup might look rather simple, it always requires careful data analysis. In principle, DWS consists in measuring the auto-correlation function of the transmitted - or backscattered - light intensity. In the limit of multiple scattering, one can consider that the photon diffuses inside the sample, with a typical mean free path l^* [23, 24]. In foams, the length l^* is a function of the bubble diameter D and liquid fraction ϕ_l : as a first approximation, $l^* \propto D/\sqrt{\phi_l}$, and corresponds typically to 2 to 4 bubble diameters [22]. Then, the intensity fluctuations arise from the dynamics occurring inside the sample. In foams, coarsening-induced rearrangements at rest, or shear-induced rearrangements result in the motion of bubbles which change neighbors. The rates of such bubble rearrangements can be determined by DWS [26].

The source of radiation is a laser (Coherent, Compass 315M-100) working at $\lambda = 533$ nm. The diffused transmitted light is collected by a monomode optical fibre (Oz Optics) equipped with a focus lens. A photomultiplier (Hamamatsu) and a correlator (Correlator.com, Flex2k-12x2) were used together with the software Flex2k (Fig.1). The duration of every measurement is 120 s. The intensity correlation function $g_2(\tau) = \frac{\langle I(\tau)I(0) \rangle}{\langle I \rangle^2}$ is measured, and the electric field autocorrelation g_1 is given by $g_2 = 1 + \beta g_1^2$, where β is the contrast [29].

As explained below, we also performed Static and Dynamic Light Scattering (SLS and DLS) on the particle suspensions. We used a home built instrument operating with a He-Ne laser (Melles Griot 75 mW) with $\lambda = 632.8$ nm. The detector is a Hamamatsu H7421-40 photon-counting head connected to a universal counter (Racal-Dana 1991) [33]. The correlator is the same Flex2k-12x2 as for DWS. Here, the scattering angle was varied from 60° to 120° .

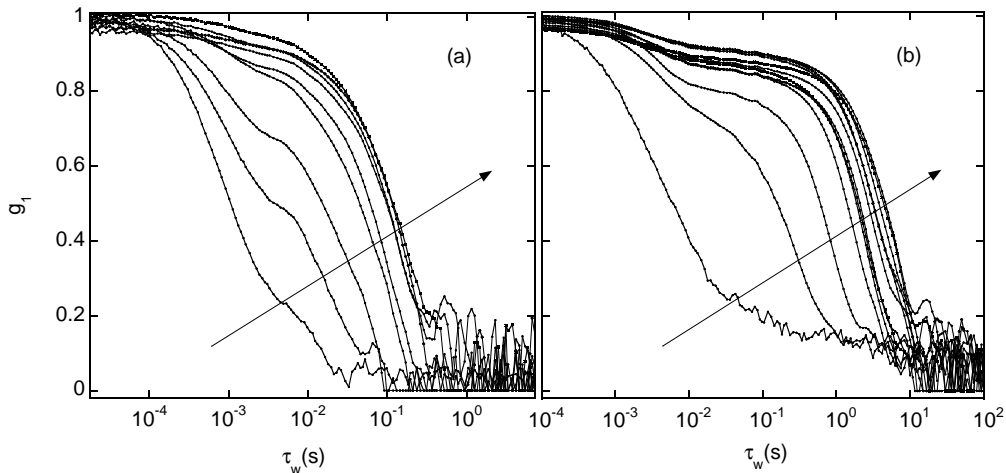


Figure 2: Correlation functions g_1 versus the delay time τ on different particle stabilized foams (a) with a particle concentration 0.3 wt%, and waiting times t_w ranging from one to 75 minutes (b) with a particle concentration 0.7 wt%, and waiting times t_w ranging from 14 minutes to 13 hours (the arrow indicates increasing t_w)

3 DWS on particle-stabilized foams : data, model and tests

3.1 Specificities of the DWS correlations curves

The effect of particle concentration on the foamability and foam stability has been recently studied [34]. In Fig.2, we show two typical sets of DWS data on foams with particle concentrations of 0.3 and 0.7 wt%, corresponding to already good enough foamability conditions. With such concentrations, the initial liquid fractions can be tuned between 0.15 and 0.3, and the measurements are made through a cell of 27 mm in thickness. The curves are given for various foam ages, or waiting times t_w , corresponding to the time elapsed since foam formation.

The correlation functions clearly show two different timescales of decay. At times τ of the order of 1 ms there is a first decay, which seems independent of the waiting time t_w . At delay times τ in the range $2 \cdot 10^{-2} - 10$ s a second decay of the correlation function is observed corresponding to another dynamical mode. This second timescale increases with the waiting time. The relative importance of the two decays also evolves with time : at a small t_w and a small concentration of particles, the fast decay is more important than at large t_w and higher solid fraction. In other words, the plateau between the two decays shifts upwards with increasing waiting

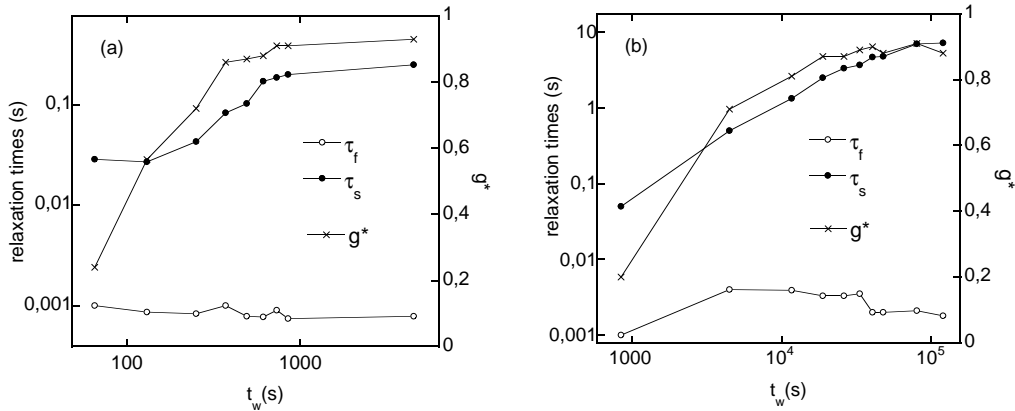


Figure 3: parameters extracted respectively from the data of Fig.2(a) and (b) : relaxation times τ_s , τ_f and plateau value g^* as a function of t_w)

time. Quantitatively, we can easily extract, by exponential fits, the values of the relaxation times for the fast and slow modes, τ_f and τ_s , for these two sets of data, and we have plotted them as a function of the foam waiting time in Fig.3. The fast relaxation time is found almost constant ; on the contrary, the slow relaxation time is approximately linear with the waiting time. We also found that the contrast β is always equal to 0.5.

Such behavior with two-modes has, to our knowledge, not been reported in multiple light scattering studies of liquid foams, where a single decay is usually observed. Note that a fast thermal dynamics has been reported, but such dynamics have features very different from what is observed here : a decay with a single characteristic time is not observed ; on the contrary, the dynamics span over many decades of delay times τ [35]. We may then expect that the origin of the fast decay observed here is a direct consequence of the presence and dynamics of solid particles in the particle-stabilized foams.

3.2 Light scattering through a particle-stabilized foam

In this section, we address the problem of the light scattered by a particle-stabilized foam. The figure 4 shows the path of a photon inside such foams. The path is composed of the succession of many scattering events. As for all foams, there is some scattering by the foam skeleton itself, i.e. the connected networks of films, Plateau borders and nodes providing a large and curved gas-liquid area. Here, the scattering arising from the foam structure is coupled to the scattering by solid

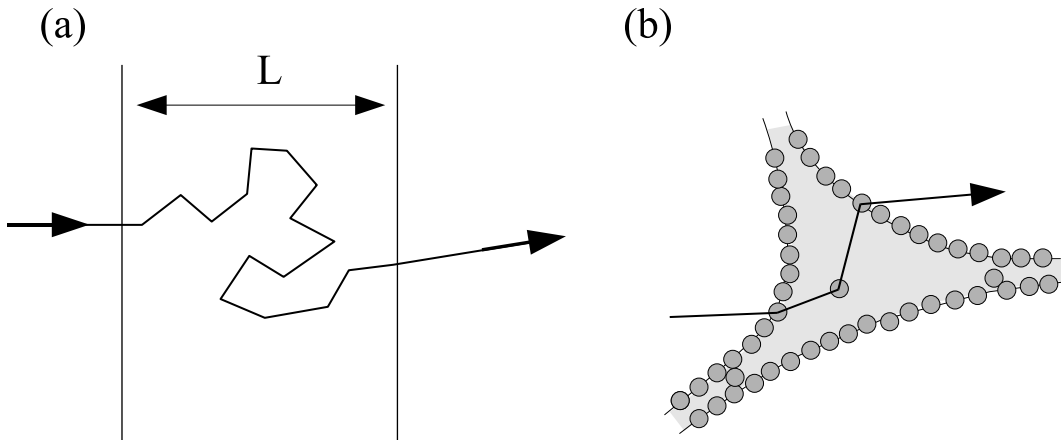


Figure 4: Sketch of the light propagation inside the foam. (a) Path of a photon propagating in a slab of foam of thickness L . (b) Zoom of a portion of a path, where the photon is scattered by solid particles.

particles adsorbed at the liquid-gas interfaces. Motions of those adsorbed particles are hindered by steric interactions and high desorption rates, and are only possible through the slow deformations of the foam skeleton. But one also has to consider some possible scattering by solid particles which are not adsorbed at interfaces. Because these particles are dispersed in the liquid phase, they are free to move and may induce a faster decay of the correlation function.

The analysis of the light scattered by a medium composed of rapidly moving particles embedded in an almost immobile scattering medium has been addressed previously; in particular, the case of light scattered by colloidal particles dispersed in a porous material has been studied [36, 37, 38]. Those authors showed that single scattering events due to the Brownian motion of these colloidal particles may be probed, although the light is multiply scattered by the porous matrix. Snabre *et al.*[27] showed that the concentration of colloidal particles may be related to the amplitude of the fast decorrelation of scattered light. We recall here briefly the principle of this analysis, and further details may be found in [27].

We consider first a path of length s for a photon propagating in the foam. Supposing that the free particles are randomly distributed in the foam, the probability that this photon is not scattered by one free solid particle is $\exp(-s/\xi_f)$. We called ξ_f the scattering length of free particles *in the foam*. Let $P(s)$ be the normalized distribution of the path lengths inside the foam. This distribution depends on the optical characteristic of the medium, as well as the geometry of light illumination and detection. The probability that a photon is not scattered by any free solid particles is then $\int P(s) \exp(-s/\xi_f) ds$. The paths with at least one scattering event with

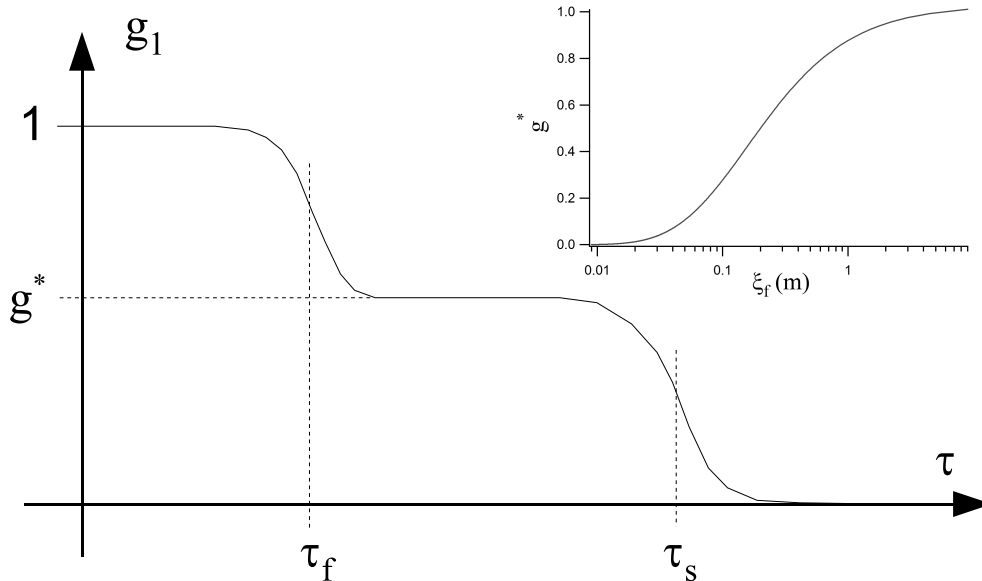


Figure 5: Typical correlation function for a system composed of fast moving particles (timescale τ_f) embedded in a medium with a slow (timescale τ_s) dynamic. Inset : value of g^* as a function of the scattering length ξ_f for a slab geometry of thickness $L = 10\text{mm}$ and a foam with a transport mean free path $l^* = 300 \mu\text{m}$.

free particles vary on a timescale related to the Brownian motion of free particles, denoted τ_f . After this time, the correlation function amplitude has decreased by $1 - g^*$, with g^* being the proportion of paths which do not have one scattering event with free particles, i.e. $g^* = \int P(s) \exp(-s/\xi_f) ds$. At longer timescales τ_s , the slow dynamics of the foam matrix takes place. This leads to a complete decorrelation of the scattered light. A typical correlation function of such a system is shown in Fig.5.

This predicted curve qualitatively corresponds to those of Fig.2, and it turns out that g^* is directly the value of g_1 on the intermediate plateau. Using the data of Fig.2, we also extracted the value of g^* and plotted it with the measured values of τ_f and τ_s (Fig.3).

3.3 Experimental test

In the theoretical framework developed in §3.2, the value of g^* depends on the scattering length ξ_f of the free particles inside the foam, and an increase of g^* corresponds to an increase of ξ_f . Thus, one should be able to deduce one quantity from the other. As a test of the model hypothesis and to check if the values of ξ_f

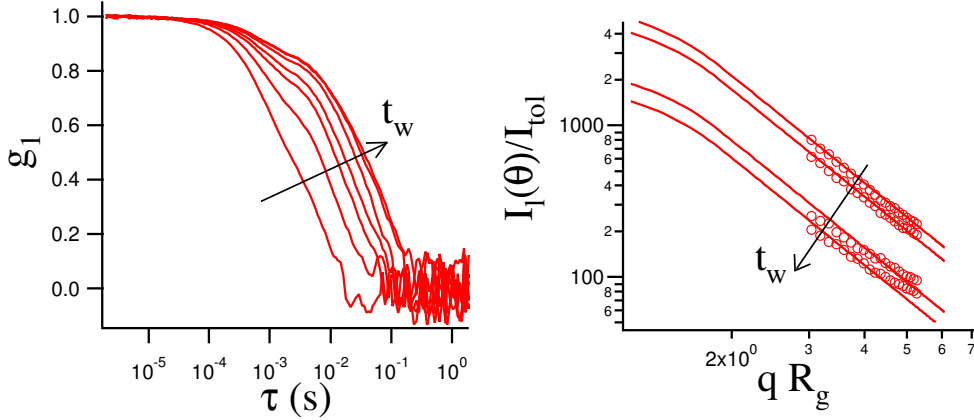


Figure 6: (a) : DWS measurements on an aging foam. Measurements are done from $t_w = 2$ min to $t_w = 14$ min, at 2 min intervals. (b) SLS measurements on the drained liquid, where (\circ) denotes the $I_l(\theta)/I_{tol}$. The full lines are the scattering model based on fractal aggregates, with q the scattering vector, and R_g the free particle radius.

deduced from g^* are correct, we performed an experiment where, simultaneously to DWS measurements, we collected samples of drained liquid at the bottom of the foam and at different waiting times. Thus, we can then directly and separately measure the scattering properties of the foam interstitial liquid itself (as it is the liquid which was previously inside the foam), and compare it to the indirect measurement made through the foam, via g^* . The figure 6 shows the results of both the DWS measurements during the foam aging (with an initial particle concentration equal to 0.7wt.%), and of the SLS measurements done on the drained liquid samples.

First, we analyze the DWS results on the foam. The value of ξ_f , which is the scattering length of free particles inside the foam (independent of the experimental setup), can be obtained from the value of the correlation function after the first decay g^* . This value is given using $g^* = \int P(s) \exp(-s/\xi_f) ds$. The distribution of path lengths $P(s)$ is obtained from the solution of the light diffusion equation with usual mixed boundary conditions at surfaces [36] and g^* is the Laplace transform of $P(s)$. In a slab geometry of thickness L , with a light transport mean free path l^* , the Laplace transform of $P(s)$ can be computed, and we get:

$$g^* = \frac{3}{5} \left(\frac{L}{l^*} + \frac{4}{3} \right) \frac{\sinh(\sqrt{K}) + \frac{2}{3} \sqrt{K} \cosh(\sqrt{K})}{\left(1 + \frac{4}{9} K \right) \sinh(\sqrt{K} \frac{L}{l^*}) + \frac{4}{3} \sqrt{K} \cosh(\sqrt{K} \frac{L}{l^*})} \quad (1)$$

with $K = 3l^*/\xi_f$. Details of the calculation of Eq.1 may be found in [27] and the references within, where the expression for g^* for a backscattering geometry

is given. We calculated g^* as a function of ξ_f using Eq.1 and show the result in the inset of Fig.5 for a slab of thickness $L = 10 \text{ mm}$ filled with a foam $l^* = 300 \text{ }\mu\text{m}$ (corresponding to the experiment of Fig.6a). From this graph, it turns out that correlation curves with two separated dynamical processes and with significant decorrelation (say, g^* around 0.5), can only be observed around $\xi_f = 0.3 \text{ m}$. It might look surprising to be sensitive to such large lengthscales (meaning very low concentrations of free particles, as discussed later) by using a cell of thickness $L = 1\text{cm}$. However, the point raised by this model is that L is not the relevant lengthscale once we deal with the foam : the relevant length to be compared to ξ_f is the mean length of the light paths inside the cell : $s \sim L^2/l^* \approx 0.3 \text{ m}$, indeed consistent with the above value of ξ_f .

From the experimental data plotted in Fig.6.a, we determine g^* at waiting times t_w . Because the time scales between the fast and the slow decay are not well separated at all waiting times, we adopt for g^* the value of the correlation function at a delay time $\tau = 2.3 \text{ ms}$. Consistently with the previous fitting results shown in Fig.3, the fast timescale is almost constant, the slow timescale increases with t_w , and g^* also smoothly increases from almost 0 to 0.9 with t_w . Using Eq.1, we then obtain ξ_f as a function of t_w . The results are plotted in Fig. 7.

Secondly, we have to analyze the results obtained using the SLS setup on the drained liquid collected at different waiting times (Fig.6.b). The scattering length of the drained solution can be obtained using SLS, by comparison of the scattered intensity of the drained liquid with the scattered intensity of a reference system of known scattering properties (Toluene). Letting I_l and I_{tol} be the scattered intensities in the vertical-vertical polarization detection, the ratio of the scattering lengths is:

$$\frac{\xi_{tol}}{\xi_l} = \frac{3}{8} \int_0^\pi \frac{I_l(\theta)}{I_{tol}} (1 + \cos^2(\theta)) \sin(\theta) d\theta \quad (2)$$

The factor $(1 + \cos^2)$ in Eq.2 takes into account polarization effects (I_{tol} is independent of θ). The scattering length of toluene ξ_{tol} is related to the tabulated value Rayleigh ratio R_{vv} accordingly to $\xi_{tol} = 3/R_{vv}8\pi$. We take $R_{vv} = 7.8 \cdot 10^{-4} \text{ m}^{-1}$ at $\lambda = 633 \text{ nm}$ from data reported in [39] at $\lambda = 647 \text{ nm}$ with a λ^{-4} correction. The ratio $I_l(\theta)/I_{tol}$ as a function of the scattering vector is plotted on Fig.6. Since the scattered intensities are measured in a limited range of scattering vectors, we need to extrapolate the scattered intensity to small and large scattering vectors. At large q we see in Fig.6 that the scattered intensity varies with $q^{-D_{F0}}$ with $D_{F0} = 2.35$. We then take at large q : $I_l \propto (qR_g)^{-D_f}$ and $I_l \propto \exp(-q^2R_g^2/3)$ at small q . The radius of gyration R_g is taken as equal to the hydrodynamic radius obtained from DLS on the drained liquid, i.e. $R_g = 230 \text{ nm}$. Interpolation between small and large q vectors is made by continuity of $I(q)$ and dI/dq . The extrapolated intensities at small and large q values are shown on Fig.6b. The integral involved in Eq.2 can be

calculated, and we finally obtain ξ_l . The values of ξ_l obtained from this analysis are then plotted on Fig.7.

4 Discussion

The comparison between the scattering length ξ_f extracted from the DWS measurements made on the foam, and the ones directly measured on the drained fluid ξ_l is shown in Fig.7. A good qualitative agreement is found ; both values increases with t_w . Concerning the quantitative comparisons, one must first remember that the free particles are only inside the foam fluid phase, not inside the gas bubbles. This implies a correction which can be implemented in different ways : for instance, taking into account the foam liquid fraction is similar to considering that the drained liquid is more dilute ; this would multiply the value of ξ_l by a factor $1/\phi_l$. Such a correction ($\phi_l \sim 0.2 - 0.3$) move the two data sets much closer. To make more accurate comparisons, one must know with precision several quantities (bubble size, l^* , ϕ_l inside the foam, as well as their evolution with time). As we do not have good accuracy on these quantities, it might become risky to push too far the quantitative comparisons. As well, one should take into account accurately the time delay corresponding to the time taken by the liquid to travel downward from the DWS measuring position to the liquid pool below the foam (here, with our experimental conditions, it is small and can be estimated to a couple of minutes). Thus at this stage, we want to point out that - including the corrections, and the estimations we can make on the foam parameters - the values of ξ_f and ξ_l are very close; and secondly, they both increase by the same factor 5 with the foam waiting time.

So, the two different and independent measurements of the scattering lengths due to free particles are consistent: this validates our interpretation of the DWS curves, as the fluid scattering properties, measured within the foam and deduced from g^* , are the correct ones. In that respect, following the model of Sec.3.2, we have thus explained the shape of the curves of Fig.2, and have demonstrated that it is due to the fact that the proportion of photon paths with no scattering event with a free particle is not exactly 100% in these foams (as described by g^*). We indeed observed the dynamics of free and fast particles embedded inside a much more slower evolving matrix. We also performed another experiment to validate our interpretation: by incorporating tiny amounts of 100nm-hydrophilic particles inside a surfactant foam, we rebuild a situation with free particles inside the liquid channels, and we know that these particles do not adsorb at interfaces. It turns out that with such a system, the same fast mode is observed and its features can also be fully explained within the theoretical framework developed here.

This agreement also confirms the non-trivial prediction that the relevant length which has to be $\simeq \xi_l$ to observe a signature of the free particles in the DWS curve is

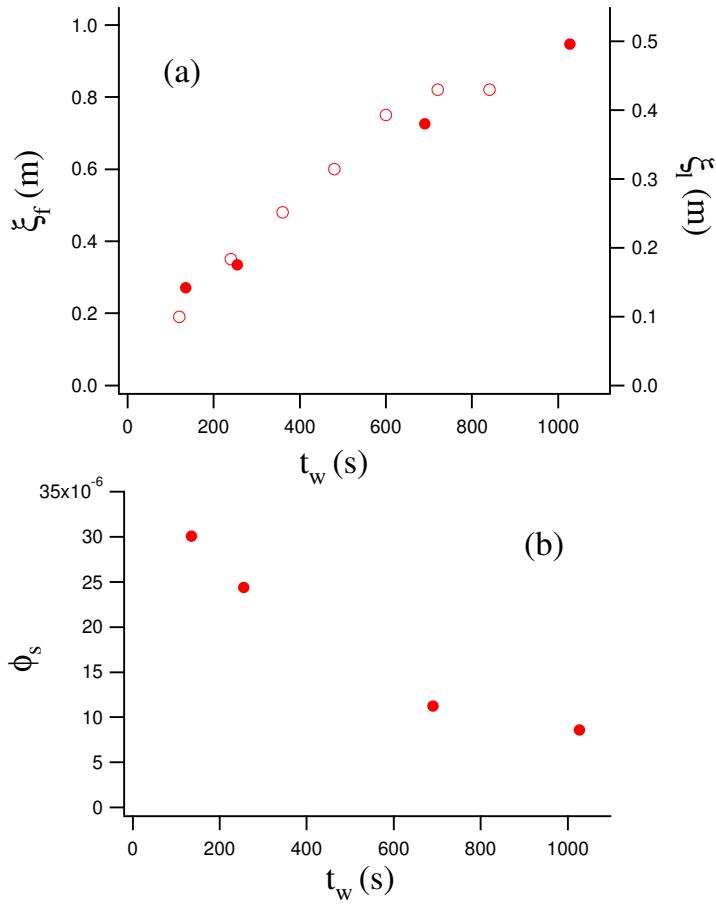


Figure 7: (a) Scattering lengths as a function of the waiting times. (o) correspond to ξ_f , describing the scattering by the free particles inside the foam, and obtained from the DWS data. (●) correspond to ξ_l , describing the scattering by the particles inside the drained liquid, obtained from SLS/DLS on the drained liquid. (b) Solid fraction in the drained liquid deduced from the scattering length of the drained liquid ξ_l and from the scattering cross section of the aggregates.

not the cell thickness L , but the photon path length $s \gg L$. Moreover, it turns out that the condition $s \simeq \xi_l$ can be seen as a criterion for obtaining a DWS curve like the one in Fig.5 with a g^* intermediate between 0 and 1. Having two well separated timescales τ_f and τ_s is therefore not sufficient to obtain the shape of Fig.5: if the fluid contains too many particles, the DWS data will be fully controlled by the fluid itself ($g^* = 0$); and if the fluid is too dilute, the particles will have no effect ($g^* = 1$). However, as s depends on L and l^* (thus, on D and ϕ_l), it is - in theory - always possible to adapt the foam and/or the setup parameters to any fluid scattering length in order to get $s \simeq \xi_l$, and $g^* \simeq 0.5$. Note also that for usual foams, one can use the fact that - due to drainage and coarsening - l^* , D and ϕ_l , and thus s , can evolve with time.

A few other quantitative remarks can be made. We already discussed the implication of the value of g^* in terms of ξ_f ; at this stage, we can also discuss the value of τ_f , and test if the short timescale seen in the DWS curves can be related to the dynamic of the free scatterers in the drained fluid. For Brownian particles, the short timescale can be expressed as [36, 38]: $\tau_f = (4D_f k^2)^{-1}$ where $k = 2\pi n/\lambda$ with n the refractive index of the medium, and D_f the diffusion constant of particles. Using the diffusion coefficient obtained from the DLS measurements on the drained liquid - $D_f = 0.94 \mu m^2.s^{-1}$ - we extract $\tau_f = 1.5 ms$, also in good agreement with the measured value of the fast decay time (Fig.3,6a). Thus, the particles diffusion constant D_f is the same if the fluid is confined in the foam or not: this means that the fast dynamics observed in the DWS curves is consistent with the free particle radius of 230 nm measured on the drained liquid. Note that this value agrees with the range of measured particle radii [31], however it corresponds to the highest values in that range. This could be due to some aggregation during the foaming process. Also, we want to point out that this analysis is based on the fact that there is only single scattering by free particles, which is correct since $s \leq \xi_l$. Consistently, we predict that the features of the fast mode must not depend on the experimental geometry (transmission or backscattering, sample size, etc...), as is the case for multiple scattering. Preliminary tests show that this is true : we recover the same value of ξ_f , for both backscattering and transmission. As τ_f does not depend on the waiting time (Fig.2), this means that the size of the aggregates remains constant. We also checked that the constant draining velocity can affect the fast relaxation timescales by no more than 1% (bubble diameters of 100 microns imply a slow drainage velocity).

The scattering length of the drained liquid is related to the concentration of free particles. The large values of ξ_l indicate that the concentration of free particles is very small. For a quantitative estimate, we can deduce the value of the solid fraction of particles in the drained liquid. The scattering cross section of fractal aggregates are discussed in the review of Sorensen [40], where many details are given. The scattering cross section of an aggregate composed of N monomers is

$\sigma_{agg} = N^2 G(kR_g) \sigma_m$ where k is the wave vector, $G(kR_g) \simeq (1 + \frac{4}{3D_f} k^2 R_g^2)^{-D_f/2}$, and σ_m is the scattering cross section of a monomer. The monomers are silica spheres of radius $a = 10nm$, and then $\sigma_m \simeq \frac{8\pi}{3} k^4 a^6 |\frac{m^2-1}{m^2+2}|^2$ with m the refractive index ratio between silica and water. The number of monomers is taken as $N = k_0 (\frac{R_g}{a})^{D_f}$, with k_0 a constant of order unity; here we took $k_0 = 3$ [40]. The number of aggregate per unit volume is then deduced from the length ξ_l as $n_{agg} = 1/\sigma_{agg} \xi_l$. The solid volume fraction in the drained liquid is then $\phi_s = n_{agg} N 4\pi a^3 / 3$. The figure 7.b shows the calculated solid volume fraction ϕ_s as a function of the waiting time, and we found $\phi_s \sim 10^{-5}$. Note that such very low values of particle volume fraction are similar to those detected by DWS in a porous material [27]. All together, one finds that g^* is linked to the concentration of free particles (decreasing with time), while τ_f is linked to the size of the aggregates (constant with time).

Concerning the evolution during foam aging, the increase of the scattering length (measured either in the foam or in the drained liquid) can only be attributed to a decrease of the concentration of free particles. Samples of drained liquid collected at the bottom of the foam, as the foam ages, are indeed more and more dilute. This means that, at a given location inside the foam and for two waiting times $t_{w1} < t_{w2}$, we have measured that there are less free particles floating in the liquid at t_{w2} than at t_{w1} . We believe that this is mostly due to the foam drainage : between t_{w1} and t_{w2} , the radius of the section of the liquid channels (the Plateau borders, where the particles are free to move) has decreased reaching typically a few microns. As a consequence of this increasing confinement, we can speculate that more and more particles can get trapped and blocked within the fluid network junctions, resulting in a decreasing effective concentration of mobile particles and thus to the increase of g^* and ξ_f .

As the time evolution is linked to drainage and to the increase of the local confinement (i.e. decrease of the local liquid fraction), and as this decrease of liquid fraction propagates downwards inside a foam [21], we understand that t_w is not an absolute parameter for comparing different data sets. In fact, depending on the initial liquid fraction, initial bubble size and the distance from the top of the sample, the drainage-induced shrinkage of the liquid channels can occur at very different waiting times. This means that qualitatively the same features (increase of g^* and ξ_f) will always occur, but not necessarily at the same foam age.

In addition, it is also possible that this increased confinement induces some further adsorption of particles. In other words, the foam drainage, which implies more confinement inside the foam, turns out to be a natural way to modify the concentration of free particles within the foam, and this allows us to test our interpretation under various conditions within a single foam.

Another explanation could be that the concentration of free particles remains constant, but as l^* increases, s decreases, automatically leading to higher g^* . How-

ever, we can rule out this effect only due to a change of the foam parameters for two reasons: first, these parameters evolve only slightly with time, and second the same increase of ξ_l is measured on the drained fluid itself (thus independent of the changes of the foam structure).

We also observe that g^* never completely reaches 1 : there are always some free particles which scatter photons. This is consistent with our macroscopic drainage observations that not all the liquid drains out of these foams, and that some solution always remains trapped inside the networks of liquid channels. In that respect, it also fits with the occurrence of particle clogging as the foam drains, making plugs within the network.

So far, we have mostly analyzed the origins of the first fast decay. The second dynamical mode, at long times, is most likely due to the foam structure itself and more usual processes, such as coarsening and coalescence. However, by measuring the mean value of the transmitted light, we observed that these particle-stabilized foams undergo almost no coarsening [13]. Indeed, we find here that the timescales of this slow mode is typically 3 orders of magnitude bigger than for usual surfactant foams (especially for the high concentration of particles, Fig.2b). Even for the lower particle concentration, the timescale remains bigger than for similar surfactant foams. Nevertheless, we have still measured a dynamics of the structure at the bubble scale : it is slow, but locally the structure is not frozen. Some rearrangements occur probably either by coarsening or coalescence (i.e. film spontaneous ruptures), and the bubble diameters evolve. Note also that the linear dependence of τ_s (Fig.3) with t_w is not consistent with a foam where only a gas-controlled coarsening occurs [25], hence coalescence likely plays an important role. As the rearrangements occurs more frequently at the lowest particle concentration and small foam ages it is possible that, at the early times, there are not yet enough particles adsorbed at the interfaces, which leads to high rates of re-organization. Then, as there are less and less bubbles, their coverage increases and finally the coarsening and/or coalescence rates becomes very small (as for Pickering emulsions). In that respect, it is reasonable that this foam structure timescale is higher for the higher particle concentration (Fig.2). These results also show the limit of measuring only the mean value of the transmitted intensity, as different bubble diameter distributions could lead to the same value. Direct measurements of the bubble diameter distributions are under progress (X-ray tomography) to clarify this picture.

This also opens some questions on what is exactly measured by DWS on foams at rest: it is usually considered that the DWS characteristic time is the time between two coarsening-induced rearrangements at a given location [26]. However, it has already been reported that in foams having very different bubble growth rates (for instance surfactant and protein foams), the DWS timescales may be very close (especially for foams with $\phi_l > 0.1$) [41]. This might be linked to the large distribution of the rate of rearrangements, the low yield strain and the large spatial

extent of rearrangements [41] and remains to be fully elucidated. In any case, it means that if one crudely considers only the DWS measurements, one might predict faster coarsening than what is actually deduced by monitoring the mean transmitted intensity. Note lastly that the slow dynamics in particle foams may not be only due to modification of the foam structure ; at this stage, we cannot rule out some other types of dynamics, like for instance the one of "slow" particles, which could be either only partially adsorbed, or adsorbed but still slowly moving along the bubble interfaces.

5 Conclusions/outlook

We have shown that DWS experiments on foams stabilized by solid particles reveal some specific features, usually not detected on surfactant foams. In particular, these foams have two independent dynamical modes, with well separated timescales and amplitudes evolving with time.

We have provided an analytical model which explains the experimental features and we propose that the first fast dynamics is the signature of single scattering by remaining free particles (i.e. not bound to the interfaces). To test this model, independent measurements of the scattering length due to the free particle - within the foam, and directly on the drained fluid itself - have been performed. The good agreement between predictions and measurements confirm the validity of our interpretation.

More interestingly, this study provides a few non-trivial results : free particles dispersed inside a foam interstitial fluid can have a strong impact on the photon correlation curves, especially at very low concentrations. We provide a criterion which gives the conditions required for observing a DWS curve with two plateaus : the length of the light path inside the foam turns out to be the important parameter to be compared to the fluid scattering length. All the features of the unusual dynamics have been explained : to summarize, the timescale depends on the free particle size, and the amplitude depends on the concentration of free particles.

These results shed light on the understanding of particle-stabilized foams: we have found that there are fewer and fewer free particles inside the foam as it ages, and that only a tiny amount of particles is not adsorbed at the interfaces. Also, even though previous work suggested that foam coarsening appears to be stopped, our results show there is always some slow dynamics within the foam (especially, at early times and low surface coverage by particles).

Our analysis should remain valid for other systems (emulsions, gels, tissues), in which a fluid containing rapidly moving scatterers is distributed within a slowly evolving diffusing matrix. The method presented might help to interpret other data where such two-modes decorrelations have been observed, but have remained

unexplained. The method could also be used to monitor very low concentrations of tracers in solutions : by foaming the solution and performing technically simple DWS, one can obtain the same information than with the more sophisticated SLS and DLS techniques.

Acknowledgements

The authors thank the financial support of the Agence Nationale pour la Recherche (ANR - grant number : ANR-BLAN-07-340). We thank Eric Raspaud for his help on the Dynamic Light Scattering experiments. We are grateful to Bernard Binks and Wacker Chemie for the gift of particles.

References

- [1] Dickinson E., *Coll. Surf. B-Biointerfaces* 1999, 15, 161.
- [2] Wilde P.J., *Current Opin. Coll. Int. Sci.* 2000, 5, 176.
- [3] Binks B.P., *Current Opinion in Colloid and Int. Science* 2002, 7, 21-41.
- [4] Tcholakova S., Denkov, N.D., Lips A., *PCCP* 2007, 10, 1608-1627.
- [5] Boker A., He J., Emrick T., *Soft Matter* 2007, 3, 1231-1248.
- [6] Pickering S.U., *J. Chem. Soc.* 1907,91,2001.
- [7] Arditty S., Whitby C.P., Binks B.P., Schmitt V., Leal-Calderon F., *Eur. Phys. J. E* 2003, 11, 273-281.
- [8] Arditty S., Schmitt V., Giermanska-Kahn J., Leal-Calderon F., *J. Coll. Int. Sci.* 2004, 275, 659-664.
- [9] Kruglyakov P.M., Taube P.R., *Colloid J.* 1972, 34, 194-196.
- [10] Bindal S.K., Sethumadavan, G., Nikolov A.D., Wasan D.T., *AIChE Journal* 2002, 48, 2307-2314.
- [11] Wilde P.J., *Adv. Colloid Interface Sci.* 1996, 64, 67-142.
- [12] Fujii S., Iddon P.D., Ryan, A.J., Armes S.P., *Langmuir* 2006, 22, 7512-7520.
- [13] Cervantes Martinez A., Rio E., Delon G., Saint-Jalmes A., Langevin D., Binks B., *Soft Matter* 2008, 4, 1531-1535.
- [14] Kam S.I., Rossen W.R., *J. Coll. Int. Sci.* 1999, 213, 329-339.
- [15] Abkarian M., Subramaniam A.B., Kim S.H., Larsen R.J., Yang S.M., Stone H.A., *Phys. Rev. Lett.* 2007, 99, 188301.
- [16] Velikov K.P., Durst F., Velev O.D., *Langmuir* 1998, 14, 1148-1155.
- [17] Subramaniam A.B., Abkarian M., Mahadevan L., Stone H.A., *Langmuir* 2006, 22, 10204-10208.
- [18] Subramaniam A.B., Mejean C., Abkarian M., Stone H.A., *Langmuir* 2006, 22, 5986-5990.
- [19] Stocco A., Drenckhan W., Rio E., Langevin D., Binks B., *Soft Matter* 2009, 5, 2215.

- [20] Tan S.N., Yang Y., Horn R.G., *Langmuir* 2010, 26, 63-73.
- [21] Saint-Jalmes, A., *Soft Matter* 2006, 2, 836-849.
- [22] Vera M.U., Saint-Jalmes, A., Durian, D., *Appl. Optics* 2001, 40, 4210-4214.
- [23] D. A. Weitz, D. J. Pine, in *Dynamic Light Scattering: The Method and Some Applications*, W. Brown, ed. Claredon, Oxford, 1993, pp. 652720.
- [24] G. Maret, *Curr. Opin. Colloid Interface Sci.* 2, 251257 1997.
- [25] Durian D.J., Weitz D.A., Pine D., *Phys. Rev. A* 1991, 44, R7902.
- [26] Gopal A.D., Durian D.J., *J. Coll. Int. Sci.* 1999, 213, 329-339.
- [27] Snabre P., Crassous J., *Eur. Phys. J. E* 2009, 29, 149-155.
- [28] *Dynamic Light Scattering: The Method and Some Applications*, edited by W. Brown (Oxford University Press, 1993).
- [29] Berne B.J. , Pecora R., *Dynamic Light Scattering With Applications to Chemistry, Biology, and Physics* (Dover Publication Inc., 2000).
- [30] Zang D., Stocco A., Langevin D., Wei B., Binks B.P., *PCCP* 2009, 11,9522-9529.
- [31] Nodstrom J., Matic A., Sun J., Forsyth M., MacFarlane D.R., *Soft Matter* 2010, DOI : 10.1039/b921488g.
- [32] Saint-Jalmes A., Vera M.U., Durian D.J., *Eur. Phys. J. B* **12**, (1999), 67.
- [33] S.Trablesi, E.Raspaud, D. Langevin, *Langmuir* **23**, (2007), 10053-10062.
- [34] Stocco A. et al, *Soft Matter* submitted.
- [35] Gopal A.D., Durian D.J., *J. Opt.Soc. Am.* 1997, 14, 150-155.
- [36] Pine D.J., Weitz D.A., Wolf P.E., Maret G., Herbolzheimer E., Chaikin P.M., in *Scattering and Localization of Classical Waves in Random Media*, edited by Sheng P., World Scientific (1990)
- [37] Rička J., *Makromol. Cgem. Macromol. Symp.* **79**,(1994) 45
- [38] Flammer I., Bucher G., Rička J., *J. Opt Soc. Am.* **A15**, (1998) 2066
- [39] Moreels E., De Ceuninck W., Finsy R., *J. Chem. Phys.***86**, (1987) 618

- [40] Sorensen C.M., *Aerosol Science and Technology* 2001, 35, 648-687.
- [41] Saint-Jalmes A., Marze S., Langevin D., in *Food Colloids 2004 : interactions, microstructure and processing*. Edited by E. Dickinson, published by the Royal Society of Chemistry, Cambridge, (2004)